

Micellar nanocarriers for anticancer drug melanin

N. M. Permyakova, T. B. Zheltonozhskaya, T. V. Beregova, D. O. Klymchuk, T. M. Falalyeyeva & L. N. Grishchenko

To cite this article: N. M. Permyakova, T. B. Zheltonozhskaya, T. V. Beregova, D. O. Klymchuk, T. M. Falalyeyeva & L. N. Grishchenko (2016) Micellar nanocarriers for anticancer drug melanin, *Molecular Crystals and Liquid Crystals*, 640:1, 122-133, DOI: [10.1080/15421406.2016.1257307](https://doi.org/10.1080/15421406.2016.1257307)

To link to this article: <http://dx.doi.org/10.1080/15421406.2016.1257307>



Published online: 14 Dec 2016.



Submit your article to this journal [↗](#)



Article views: 3



View related articles [↗](#)



View Crossmark data [↗](#)

Micellar nanocarriers for anticancer drug melanin

N. M. Permyakova^a, T. B. Zheltonozhskaya^a, T. V. Beregova^b, D. O. Klymchuk^c, T. M. Falalyeyeva^b, and L. N. Grishchenko^a

^aTaras Shevchenko National University of Kyiv, Faculty of Chemistry, Department of Macromolecular Chemistry, Kyiv, Ukraine; ^bTaras Shevchenko National University of Kyiv, ESC "Institute of Biology", Kyiv, Ukraine; ^cInstitute of Botany, National Academy of Sciences of Ukraine, Kyiv, Ukraine

ABSTRACT


The effective biocompatible and partially biodegradable micellar nanocarriers for encapsulation of the anticancer drug eumelanin were created. Such nanocarriers are the products of self-assembly of asymmetric diblock and triblock copolymers, which comprised chemically complementary (methoxy)poly(ethylene oxide) and poly(acrylic acid) blocks of a variable length. A chemical structure and solubility of the eumelanin, the vital activity product of black yeast "*Nadsoniella nigra* sp. X-1", was characterized. Peculiarities of the micellization process, morphology, size and stability of the developed micellar nanocarriers were highlighted. The eumelanin encapsulation into micellar nanocarriers with different morphology and a state of the obtained drug/micelle systems were studied and discussed.

KEYWORDS

block copolymer;
intramolecular polycomplex;
micelle; eumelanin;
encapsulation

Introduction

Various pharmaceutical nanocarriers, such as liposomes, lipoproteins, microemulsions, polymeric micelles, nanocapsules and nanoparticles are widely used for delivery of therapeutic drugs to enhance their efficacy [1–4]. The application of micelle-type polymeric nanocontainers is considered as one of the most perspective ways to encapsulate poorly soluble and toxic compounds and to deliver them into certain cells of living organisms. Amphiphilic block copolymers with thermodynamically immiscible hydrophobic and hydrophilic blocks can self-assemble into the "core/corona" micelle structures in selective solvents [5]. An increasing number of publications proved a high efficacy of such micellar systems formed by amphiphilic block copolymers and contained hydrophobic drugs [5,6]. At the same time, it is relatively difficult to obtain such micellar systems in aqueous medium [5,6]. We reported recently that the double hydrophilic block copolymers MOPEO-*b*-PAAc and PAAc-*b*-PEO-*b*-PAAc with the system of cooperative hydrogen bonds between chemically complementary (methoxy)poly(ethylene oxide) and poly(acrylic acid) blocks formed stable micelles in aqueous medium at pH < 5 [7,8]. These micelles contained hydrophobic complex "core" with H-bonded segments of interacting blocks and hydrophilic "corona" included free (unbound) segments of longer blocks. Several of these micellar carriers were successfully used for delivery of hydrophobic drug α -tocopherol acetate (α -TOCA), commonly known as analog of Vitamin E [8]. The encapsulated α -TOCA provided *in vivo* its full assimilation by animals (white mice),

CONTACT N. M. Permyakova  permyakova@ukr.net

Color versions of one or more of the figures in the article can be found online at www.tandfonline.com/gmcl.

© 2016 Taylor & Francis Group, LLC

high efficacy due to a long-time circulation in their organisms and the reduction in its therapeutic concentration in 25 times [9]. The current work is dedicated to application of such micellar nanocarriers based on MOPEO-*b*-PAAc diblock and PAAc-*b*-PEO-*b*-PAAc triblock copolymers (DBC and TBC) for encapsulation of anticancer drug eumelanin (EMel) [10].

The melanins are a broad class of functional biopolymers found throughout in nature [10–14]. In human skin melanin appears in two forms: eumelanin and pheomelanin. The most widely accepted function of melanin in skin is photoprotection. A heavily pigmented skin with high levels of EMels, the black insoluble biopolymers produced by cutaneous melanocytes, is the indicator of an efficient protection against the damaging effects of intensive or chronic sun exposure and a lower susceptibility to melanoma and other aggressive forms of skin cancer [10]. EMel biopolymers are poorly soluble in water, that had limited its usefulness in intravenous solutions, and biologically unstable when exposed to environmental factors such as light, temperature, and oxygen. The current work presents a detailed study of chemical structure, solubility, electrochemical and absorption properties of EMel sample, which is the vital activity product of black yeast “*Nadsoniella nigra* sp. X-1 [14]. Aqueous micellar solutions of the copolymers were used here as nanocontainers for encapsulation of the EMel sample. The EMel connection under the effect of DBC and TBC molecular structure and the changes in morphology, size, and stability of their micelles without and with this drug was considered. The nature of bonds, which are responsible for EMel interaction with the copolymer micelles, was also estimated.

Experimental

Eumelanin characterization

Chemical structure of EMel sample, which was the vital activity product of black yeast “*Nadsoniella nigra* sp. X-1” [14], was studied by ^1H NMR and FTIR spectroscopy. ^1H NMR spectrum of EMel was recorded on a Varian Mercury-400 instrument at 20°C in DMSO- d_6 ($C_{\text{EMel}} = 1 \text{ kg}\cdot\text{m}^{-3}$). Determination of the chemical shift values (δ) was carried out relatively to proton signal of tetramethylsilane. FTIR spectra of thin ($\sim 10 \mu\text{m}$) films of EMel were measured by a Nexus-470 Nicolet spectrometer (USA) in the range of $1000\text{--}4000 \text{ cm}^{-1}$ at 20°C . The films were cast on fluorite windows, air-dried and then maintained in vacuum desiccator above CaCl_2 during one week.

Electrochemical properties of EMel in aqueous solution were studied by potentiometric titration. EMel suspension in water ($C = 1 \text{ kg}\cdot\text{m}^{-3}$) was prepared exactly in the thermostatic cell and then was fully dissolved by the addition of NaOH ($C = 2 \text{ mol}\cdot\text{m}^{-3}$) up to $\text{pH} \sim 11$. Potentiometric titration of fully dissolved EMel sample was performed with HCl ($C = 2 \text{ mol}\cdot\text{m}^{-3}$) up to $\text{pH} = 2$ in argon current at $T = 25 \pm 0.1^\circ\text{C}$ using a 1–160M pH-meter (Belarus) calibrated with the standard buffer solutions.

Determination of the main parameters and morphology of the copolymer micelles

Two series of DBCs and TBCs with a variable length of both the blocks were synthesized using a template radical block copolymerization process as was described in our previous works [7,8]. For this purpose we used one sample of metoxypoly(ethylene glycol) ($M_n = 5.3 \text{ kDa}$), two samples of poly(ethylene glycol) ($M_n = 6.0$ and 35.0 kDa) from “Fluka” (USA), and monomer acrylic acid from “Aldrich” (USA). Terminal hydroxyl groups of (MO)PEG were activated in these syntheses by cerium ammonium nitrate [15]. Chemical structure and

Table 1. Molecular parameters of the block copolymers.

Sample	$M_{n(\text{MO})\text{PEO}}$, kDa	$M_{n\text{PAAc}}$, kDa	$M_{n\text{DBC/TBC}}^{\text{a)}}$, kDa	$n^{\text{b)}}$
DBC1	5.3	9.3	14.6	1.1
DBC2	5.3	17.6	22.9	2.0
TBC1	6.0	5.8	17.6	0.6
TBC2	35.0	28.3	91.6	0.5

^{a)} $M_{n\text{DBC}} = M_{n\text{MOPEO}} + M_{n\text{PAAc}}$; $M_{n\text{TBC}} = M_{n\text{PEO}} + 2 \cdot M_{n\text{PAAc}}$.

^{b)} The ratio between units of PAAc and (MO)PEO blocks.

molecular parameters of the copolymers were characterized by ^1H NMR spectroscopy as in the study [7,16] (Table 1). Thus, two series of asymmetric DBCs with the constant length of MOPEO block and growing length of PAAc block as well as asymmetric TBCs with increasing length of both the blocks were obtained.

Self-assembly of DBCs and TBCs in aqueous medium as a function of the solution pH was investigated using static light scattering. For this purpose, a modernized instrument FPS-3 (Russia) contained a light-emitting diode ($\lambda = 520$ nm) from “Kingbright”, an ADC-CPUTM controller from “Insoftus” (Ukraine) and the computer program WINRECORDER were used.

Morphology and size of the copolymer micelles were established by transmission electron microscopy (TEM). TEM images of copolymer micelles were obtained with a JEM-I230 instrument (“JEOL”, Japan) operating at an accelerating voltage of 90–100 kV. Small drops ($\sim 1 \cdot 10^{-4}$ cm³) of DBC and TBC solutions ($C = 0.5 \div 1$ kg·m⁻³) in the deionized water at a necessary pH were deposited in copper grids coated with Formvar film and carbon and then were dried on air for ~ 1 –2 min and in vacuum desiccator for 24 h.

Studies of eumelanin encapsulation by the copolymer micelles

Characterization of EMel interaction with the copolymer micelles at different conditions was carried out by UV-Vis and FTIR spectroscopy as well as by TEM. UV-Vis spectra of the EMel/copolymer mixtures and pure components were recorded in the 200–1000 nm region using a Cary 50 Scan UV-Visible spectrophotometer from “Varian” (USA). FTIR spectra of thin films of the mixtures and pure components were obtained as was described above. TEM images of TBC composition with EMel were obtained using the above-described methodology.

Results and discussion

Chemical structure of eumelanin

Melanin appears to be a polymer of specific known monomers, but that may not be a definite polymer structure at all. Melanin rather appears to be composed of a variety of oligomeric components put together in various random ways, making up a final structure, which is characterized to a significant extent by structural and chemical disorder [10–13]. Biosynthetically, EMel biopolymers arise within organelles termed melanosomes by tyrosinase-catalyzed oxidation of tyrosine via oxidative polymerization of 5,6-dihydroxyindole (DHI), 5,6-dihydroxyindole-2-carboxylic acid (DHICA) and other biosynthetic intermediates [10–13]. The oxidative polymerization process involves the generation of extremely complex mixtures of oligomeric species at various levels of oxidation and degrees of polymerization, linked through diverse bonding patterns depending on the nature of the precursors and featuring

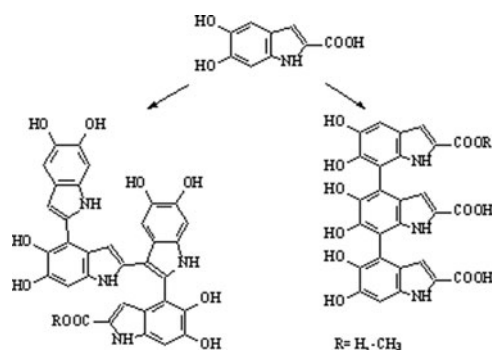


Figure 1. Building blocks of EMel based on DHICA.

apparent molecular weights up to 4 kDa. As polymerization proceeds, the aggregation processes and deposition of black insoluble particles within the melanosomes become significant and determine the complex organization of EMel biopolymers (Fig. 1). Thus, the black to brown EMel is now generally accepted to be highly heterogeneous macromolecules based on DHI and DHICA units and their oxidized states coupled in oligo- and polymeric structures.

The existence in EMel macromolecules of indol aromatic rings (they ensure an intense proton signal with the chemical shift $\delta = 7.44$ ppm), phenol hydroxyl groups (they show a weak proton signal with $\delta = 8.15$ ppm) and some ester groups $-\text{OCOCH}_3$ (they demonstrate weak proton signals with $\delta = 1.23, 1.38,$ and 1.95 ppm), which formed instead of carboxylic ones, was established by ^1H NMR spectroscopy [10,17] (Fig. 2 a). In FTIR spectrum of EMel thin film prepared at pH = 6.17 we observed $\nu_{\text{sc}=\text{O}}$ and $\nu_{\text{asC}=\text{O}}$ vibration bands for the negatively charged $-\text{COO}^-$ groups at 1406 and 1507 cm^{-1} correspondingly, and also three overlapped bands of the charged $>\text{NH}_2^+$ groups at $\sim 2040, \sim 2600$ and $\sim 2850\text{ cm}^{-1}$ (Fig. 2 b). So the zwitter-ionic character of EMel macromolecules due to a presence of the oppositely charged amine and carboxylic groups in a solid sample was revealed. This method showed also numerous hydrogen bonds formed evidently between hydroxyl and carboxylic groups of EMel. Such conclusion was confirmed by the presence of $\nu_{\text{O-H}}$ vibration band of the bonded $-\text{OH}$ groups at 3394 cm^{-1} and 3155 cm^{-1} .

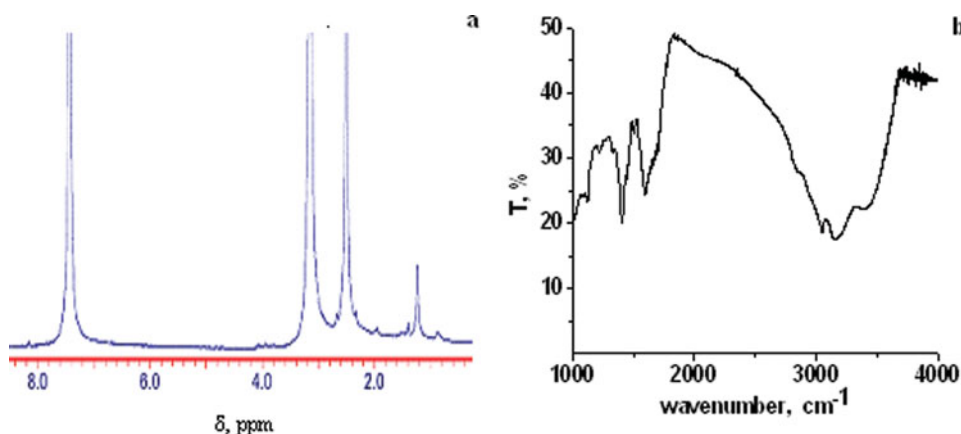


Figure 2. (a) ^1H NMR spectrum of EMel in DMSO-d_6 ; $C = 1\text{ kg}\cdot\text{m}^{-3}$. (b) FTIR spectrum of thin film ($\sim 10\text{ }\mu\text{m}$) of EMel cast from aqueous solution at pH = 6.17 on fluorite window. $T = 20^\circ\text{C}$.

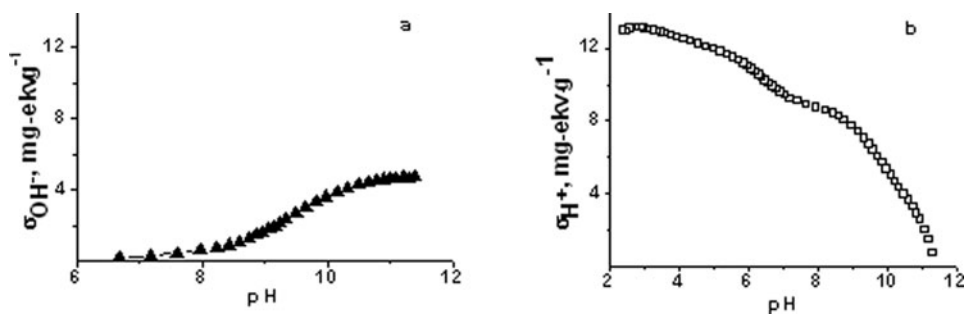


Figure 3. Dependences of the values of (a) hydroxyl absorption and (b) proton absorption vs pH in EMel aqueous solution. $C = 1 \text{ kg} \cdot \text{m}^{-3}$, $T = 25^\circ\text{C}$.

A state and solubility of eumelanin in aqueous media

It is known that melanins are dissolved in water solution only at $\text{pH} \geq 10$ [14]. Their polyampholyte properties could be clearly displayed in the process of potentiometric titration. That is why we carried out potentiometric titration of our EMel sample using a special procedure described above. The results of potentiometric titration EMel aqueous suspension by NaOH and the obtained at $\text{pH} \sim 11.5$ aqueous solution by HCl are shown in Figure 3.

They were represented as the hydroxyl absorption curve (Fig. 3 a) and the proton absorption curve (Fig. 3 b), which were calculated using well-known method [18]. The curve in Figure 3 b demonstrate the region of so-called “the minimum buffer capacity” at $\text{pH} \sim 8$, which one determine the end of protonation for EMel amine groups and the protonation beginning for the charged $-\text{COO}^-$ groups [18]. This fact allows calculating the quantity of carboxylic and amine groups in our EMel sample. Thus, some excess (in 7 mol %) of secondary amine groups against carboxylic ones was determined by this method. Acidic properties of both the groups were characterized from corresponding dependences of negative logarithm of the effective dissociation constant versus the dissociation degree, $\text{pK} = f(\alpha)$, which were calculated from the absorption curve in Figure 3 b using well-known methodology [18]. These data are shown in Figure 4.

We carried out further extrapolation of the $\text{pK} = f(\alpha)$ curves to $\alpha = 0$ and found the values of pK_0 (a negative logarithm of the intrinsic dissociation constant) for carboxylic (4.44) and amine (9.27) groups. An interesting phenomenon of a strong compaction of EMel macrocoils was revealed by the analysis of the curve in Figure 4 a. Really, relatively sharp increase in the slope of this curve in a region of $\alpha < 0.5$ ($\text{pH} < 6$) pointed out a strengthening electrostatic interactions between neighboring groups in EMel macromolecules due to their compression. The

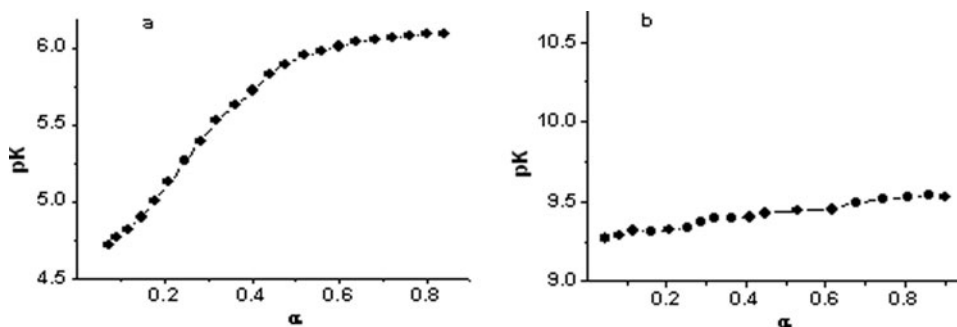


Figure 4. Dependences of pK vs α for: (a) carboxylic and (b) secondary amine groups of EMel.

Table 2. Thermodynamic parameters for the block copolymer micelles.

Sample	n	pH	CMC·10 ⁶ , mol·dm ⁻³	-ΔG°, kJ·mol ⁻¹
DBC1	1.1	2.5	4.10	30.4
DBC2	2.0	2.5	4.20	30.4
TBC1	0.6	3.5	4.70	30.1
TBC2	0.5	4.0	1.80	32.4

main reason for such effect is evidently formation of the developed H-bond system between uncharged -COOH groups and phenolic -OH groups in this pH interval.

The copolymer micellization as a function of the solution pH

Considered copolymers with hydrophilic asymmetric chemically complementary components form stable micelles in dilute aqueous solutions at pH ≤ 4 for DBCs and pH < 5 for TBCs [7,9]. Their self-assembly take place due to: i) formation of intramolecular polycomplexes (IntraPCs) in the copolymer macromolecules and ii) segregation of hydrophobic bound segments of some IntraPCs [7]. Such micelles contain hydrophobic complex “core” with H-bonded segments of interacting (MO)PEO and PAAc blocks and hydrophilic “corona” with free (unbound) segments of longer blocks. The micellization process in DBC and TBC aqueous solutions develops only at low pH due to protonation of -COO⁻ groups of PAAc blocks, which participate in hydrogen bonding, followed by hydrophobic interactions between non-polar bound segments of both the blocks [7,19].

Parameters of the micellization process and micelle stability at pH < 5, namely: the critical micellization concentrations (CMCs) and the Gibbs free micellization energies (-ΔG°) were calculated using the data of static light scattering and the relation: $\Delta G^\circ = RT \ln \text{CMC}$ [20] (Table 2).

Comparing the relative length (n) of (MO)PEO and PAAc blocks, one could assume that DBC1 macromolecules formed spherical “crew-cut” micelles [20] contained in addition to hydrophobic “core” with H-bonded segments of both the blocks also a small “corona” consisted of short unbound segments of PAAc blocks (the upper part of Fig. 5 a). The alternative micelle structure could be attributed to DBC2, which comprised a double excess of

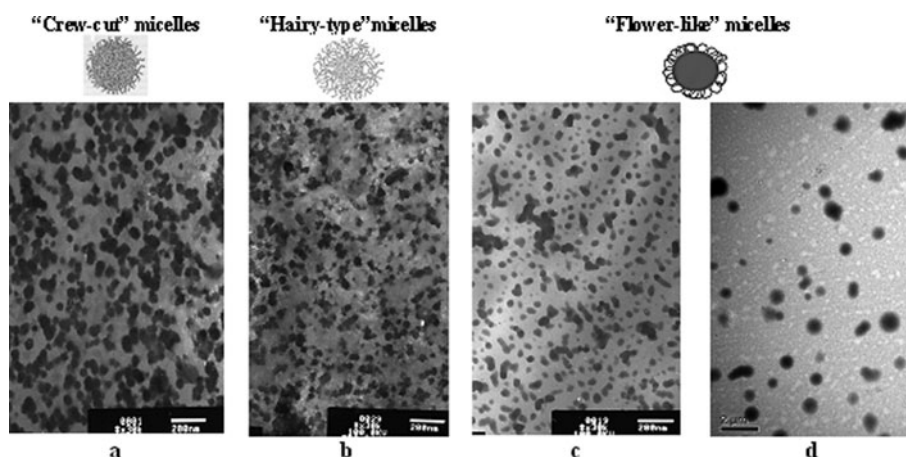


Figure 5. Schematic building of the “crew-cut”, “hairy-type” and “flower-like” micelles and also TEM images of (a) DBC1, (b) DBC2, (c) TBC1, and (d) TBC2 micelles at pH = 2.5. $C_{\text{DBC2/TBC2}} = 0.5 \text{ kg} \cdot \text{m}^{-3}$ (a, b, d), $C_{\text{TBC1}} = 1 \text{ kg} \cdot \text{m}^{-3}$ (c).

Table 3. Diameters of the block copolymer micelles.

Sample	C, kg · m ⁻³	pH	d _{MMM} ^{a)} , nm	d _{PMM} ^{b)} , nm
DBC1	0.5	2.5	4÷8	12÷68
DBC2	0.5	2.5	2÷4	8÷31
TBC1	1	3.5	4÷16	24÷58
TBC2	0.5	3.5	4÷16	270÷1280

^{a)}The diameter of monomolecular micelles.

^{b)}The diameter of polymolecular micelles.

PAAC units. In this case, the formation of “hairy-type” micelles with a large “corona” would be expected [5] (the upper part of Fig. 5 b). In the cases of TBCs, the micellization process developed due to H-bonding two shorter terminal PAAC blocks with nearest parts of PEO central block. Therefore, the appearance of other “flower-like” micelles would be waiting. Insoluble “tails” of TBCs would self-assemble in water in micelle “cores”, while soluble “loops” of PEO would be concentrating in micelle “coronas” [21] (the upper part of Fig. 5 c, d). According to Table 2, the highest stability in aqueous solution is characteristic for TBC2 micelles because for this copolymer sample the lowest CMC and the largest $-\Delta G^\circ$ values were obtained.

Morphology of the block copolymer micelles

Different morphology of the micelles depending on asymmetric character of the block copolymers was confirmed by TEM (Fig. 5). All TEM images demonstrated as polymolecular micelles (PMMs) and their separate aggregates as monomolecular-type micelles (MMMs), which were displayed as small dark points and were in fact individual IntraPCs. But morphology and size of PMMs were essentially different for DBC and TBC samples (Fig. 5, Table 3).

Polymolecular micelles of DBC1 really had relatively large “core” and short “corona” (Fig. 5 a), which form a very uneven shell at the “core” surface. The micelles of DBC2 were differed by large diffusive “coronas” (Fig. 5 b), which could be observed at a strong image magnification. The polymolecular “flower-like” micelles of both TBCs showed the most “smooth” surface (Fig. 5 c, d) because their “coronas” were made up by “loops” of PEO central blocks.

Dimensions of the DBC1, DBC2 and TBC1 polymolecular micelles were relatively small (from 8 to 68 nm) as compared to those for TBC2 micelles (270÷1280 nm). Such difference is conditioned, on the one hand, by the longest sequences of H-bonded units between PAAC and PEO blocks in TBC2 that is by the longest “hydrophobic blocks”, which determine the largest size of micelle “core”, and on the other hand, by the most lengthy chains of the surplus (unbound) PEO units, which form the largest “loops” in the micelle “corona.” Appearance of the largest TBC2 micelles in water was fully correlated with their highest stability in this medium (Table 2).

Thus, a wide spectrum of morphological forms of the given micellar carriers could be produced by variation of the absolute and relative length of both the blocks. The presence of complex “core”, which is stabilized by both the hydrogen bonds and hydrophobic interactions, allow assuming a high binding capability of such micelles with respect to different drugs of hydrophobic and hydrophilic origin [3,7,9].

Eumelanin connection by the copolymer micelles with different morphology

Homogeneous EMel/copolymer mixtures with the relative ratio $\varphi = 0.01 \text{ mol}_{\text{EMel}}/\text{base-mol}_{\text{PAAC}}$ were produced by the addition of a small volume (7.0 v %) of EMel aqueous solution

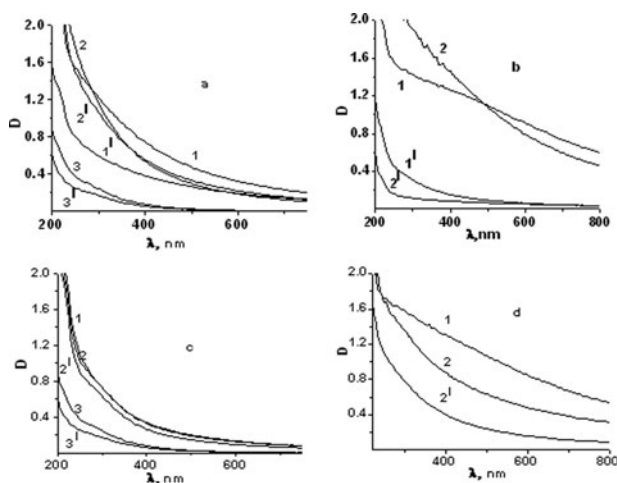


Figure 6. Extinction spectra for aqueous solutions of pure DBCs -1,1', EMel/DBC mixtures -2,2' and pure EMel -3,3' recorded through 1 h (1, 2, 3) and 24 h (1', 2', 3'). The spectra relate to: (a, b) DBC1 and its mixture with EMel, and (c, d) DBC2 and its composition. $C_{\text{DBC}} = 1 \text{ kg} \cdot \text{m}^{-3}$; $C_{\text{EMel}} = 1.63 \cdot 10^{-2}$ (a, b) and $1.67 \cdot 10^{-2} \text{ kg} \cdot \text{m}^{-3}$ (c, d); $\varphi = 0.01 \text{ base-mol}_{\text{EMel}}/\text{base-mol}_{\text{PAAc}}$. $\text{pH}_{\text{mix}} = 3.5$ (a, c) and 3.0 (b, d). $T = 22^\circ \text{C}$.

($\text{pH} = 11$) to a large volume (93.0 v %) of the copolymer solution. Since the micellization processes in DBC and TBC solutions were pH-sensitive [7], the EMel encapsulation we studied at two acidic pH values equaled to 3.5 and 3.0, which corresponded to weaker and stronger copolymer micelles.

Extinction spectra of pure DBCs at $\text{pH} = 3.5$ and 3.0 , pure EMel at $\text{pH} = 2.6$ and EMel/DBC mixtures at two pointed pH, which ones were recorded in different time (1 h and 24 h) after every solution preparation, are represented in Figure 6. It is seen that pure components (DBC and EMel) have no any absorption bands in the extinction spectra in a region of $\lambda > 400 \text{ nm}$; therefore, we could use the values of optical density (D) at $\lambda = 500 \text{ nm}$ to characterize the changes in the solution turbidity at different conditions.

So, the addition of EMel to solutions of both DBCs containing weaker micelles ($\text{pH} = 3.5$) did not result in essential changes in a micelle state (Fig. 6 a, c; curves 2, 2'). The system remained stable in time and showed only a weak opalescence. Unlike this, in acidic EMel solution, sediment appeared in a measuring cell through 24 h that was accompanied by a sharp decrease in the optical density (turbidity) of the solution (Fig. 6 a, c; curves 3, 3'). Other picture was observed in both the systems at $\text{pH} = 3.0$ (Fig. 6 b, d; curves 2, 2'). The introduction of EMel to DBC solutions contained stronger micelles initiated micelle aggregation followed by a phase separation in both the systems in time. This process was accompanied by sediment arising after 24 h and a sharp reduction in the solution turbidity. It was established that the EMel/DBC2 mixture was more stable in time than the EMel/DBC1 one because of existence evidently more developed stabilizing “corona” in the “hairy-type” micelles of DBC2.

Situation in the case of EMel addition to TBC solutions at $\text{pH} = 3.5$ and 3.0 is reflected in Figure 7. Here, the TBC1 and TBC2 “flower-like” micelles demonstrate different behavior. Indeed, the solutions of TBC1 and EMel/TBC1 mixture turned out to be instable in time at both pH values that is why sediment of pure TBC micelles or corresponding composition appeared in a cell through 24 h. This resulted in a sharp lowering the optical density of both solutions (Fig. 7 a, b; curves 1, 1' and 2, 2'). Unlike this, TBC2 micelles showed relatively high stability in time at both pH values (Fig. 7 c, d; curves 1, 1') but after EMel introduction at

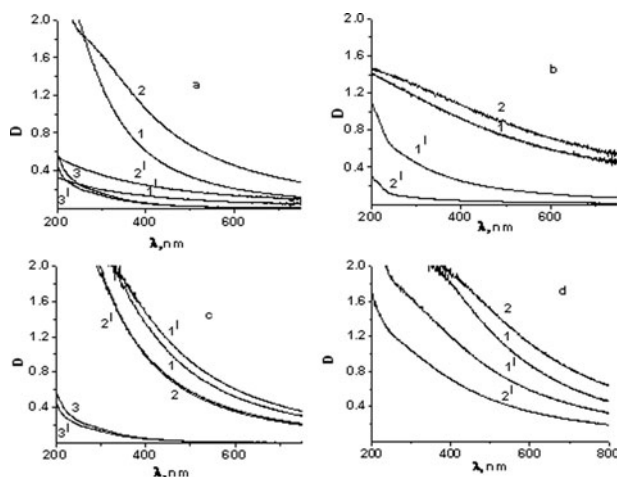


Figure 7. Extinction spectra for aqueous solutions of pure TBCs -1,1', EMel/TBC mixtures -2,2' and pure EMel -3,3' recorded through 1 h (1, 2, 3) and 24 h (1', 2', 3'). The spectra relate to: (a, b) TBC1 and its mixture with EMel, and (c, d) TBC2 and its composition. $C_{\text{DBC}} = 1 \text{ kg} \cdot \text{m}^{-3}$; $C_{\text{EMel}} = 1.46 \cdot 10^{-2}$ (a, b) and $1.39 \cdot 10^{-2} \text{ kg} \cdot \text{m}^{-3}$ (c, d); $\varphi = 0.01 \text{ base-mol}_{\text{EMel}}/\text{base-mol}_{\text{PAAc}}$; $\text{pH}_{\text{mix}} = 3.5$ (a, c) and 3.0 (b, d). $T = 22^\circ \text{C}$.

$\text{pH} = 3.0$ a phase separation through 24 h took place also (Fig. 7 d; curves 2, 2'). Nevertheless, the same mixture at $\text{pH} = 3.5$ was fully stable in time (Fig. 7 c; curves 2, 2').

The nature of EMel interaction with DBC and TBC micelles was established by FTIR spectroscopy. FTIR spectra of thin films of pure EMel in acidic aqueous solution ($\text{pH} = 2.6$), pure DBC2 in acidic aqueous solution ($\text{pH} = 2.75$) and EMel/DBC2 mixture at $\text{pH} \sim 3$ in two most important regions of (a, c, e) $\nu_{\text{C}=\text{O}}$ and (b, d, f) $\nu_{\text{C-H}}$, $\nu_{\text{N-H}}$, $\nu_{\text{O-H}}$ vibrations are shown in Figure 8. In FTIR spectrum of pure EMel ($\text{pH} = 2.6$) an intense asymmetric band of $\nu_{\text{C}=\text{O}}$ vibrations at $\sim 1710\text{--}1720 \text{ cm}^{-1}$ was observed (Fig. 8 a). It could be attributed firstly to the uncharged $-\text{COOH}$ groups, which form H-bonds evidently with biphenol hydroxyl groups. Also this band would contain $\nu_{\text{C}=\text{O}}$ vibrations of two neighbor carbonyl groups connected in EMel molecule with benzene ring of indol fragment. According to the spectral atlas [17], this band would be displayed at 1669 cm^{-1} ; therefore, by its appearance the asymmetric character of the band at $\sim 1710\text{--}1720 \text{ cm}^{-1}$ could be explained. In the pointed region there are also two characteristic bands of $\nu_{\text{sC}=\text{O}}$ and $\nu_{\text{asC}=\text{O}}$ vibrations at ~ 1410 and $\sim 1600 \text{ cm}^{-1}$ consequently, which are conditioned by the formation of zwitter-ions in the EMel polyampholyte molecules. The existence of zwitter-ions is confirmed additionally by the strongly overlapped $\nu_{\text{N-H}}$ vibration bands at ~ 2040 , ~ 2600 , and $\sim 2850 \text{ cm}^{-1}$ (Fig. 8 b) that correspond to the charged amine groups of indol [17]. The fragment of FTIR spectrum in Figure 8 b indicate also the presence in EMel macromolecules a great number of H-bonds with participation of phenolic hydroxyls and carboxylic groups. Indeed, two bands of $\nu_{\text{O-H}}$ vibrations at ~ 3200 and $\sim 3400 \text{ cm}^{-1}$ confirm such conclusion.

The spectrum of pure DBC2 ($\text{pH} = 2.75$) contain an intense $\nu_{\text{C}=\text{O}}$ vibration band of the uncharged $-\text{COOH}$ groups of PAAc block at 1720 cm^{-1} (Fig. 9 c), which form H-bonds with each other (such as "cyclic dimmers") and also with oxygen atoms of MOPEO block [17]. A wide $\nu_{\text{O-H}}$ vibration band in the range of $2600\text{--}2700 \text{ cm}^{-1}$ points out the existence H-bonds of the first type but the H-bond formation of the second type is confirmed by the $\nu_{\text{O-H}}$ vibration band of bound hydroxyls near 3200 cm^{-1} (Fig. 8 d).

Analysis of FTIR spectrum of the mixture EMel/DBC2 ($\text{pH} \sim 3$) showed the appearance side by side with intense band of $\nu_{\text{C}=\text{O}}$ vibrations of bound $-\text{COOH}$ groups also the band

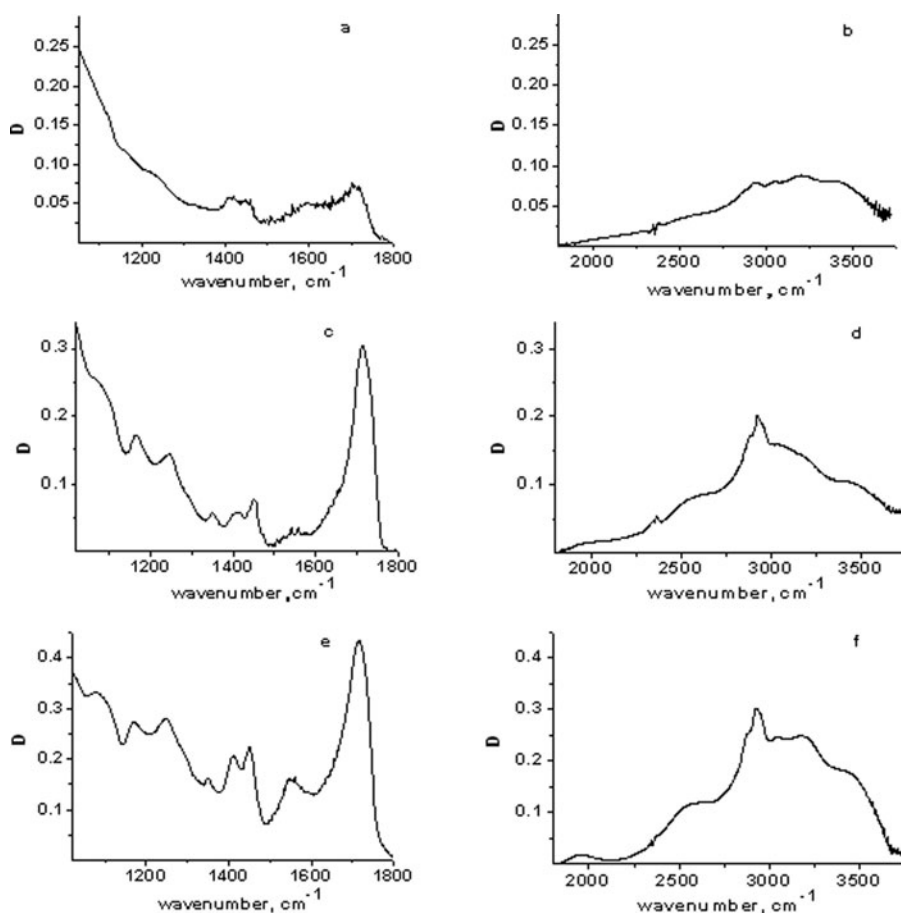


Figure 8. FTIR spectra of thin films ($\sim 10 \mu\text{m}$) cast on fluorite windows for: (a, b) pure EMel (pH = 2.6), (c, d) pure DBC2 (pH = 2.75) and (e, f) EMel/DBC2 mixture (pH ~ 3.0). $T = 20^\circ\text{C}$.

with the average intensity at $1540\text{--}1550 \text{ cm}^{-1}$ (Fig. 8 e). It could be attributed (taking into account the presence also the second characteristic band at $\sim 1410 \text{ cm}^{-1}$) to $\nu_{\text{asC=O}}$ vibrations of --COO^- ions [17]. At the same time, in the spectrum of EMel/DBC2 mixture (unlike to the spectrum of pure EMel), essentially lower distance Δ between positions of $\nu_{\text{SC=O}}$ and

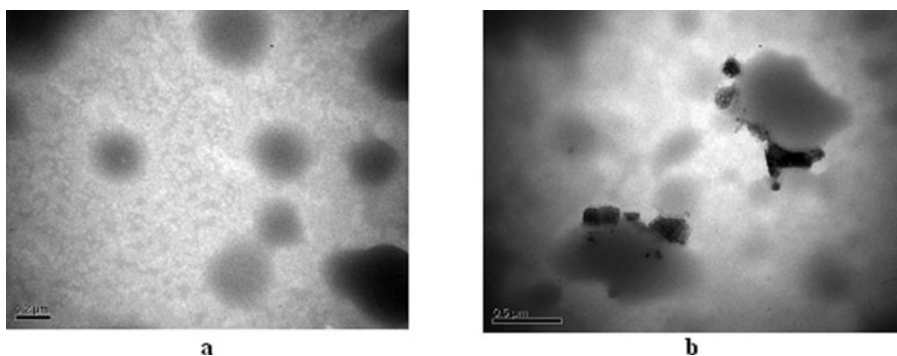


Figure 9. TEM images of: (a) free TBC2 micelles and (b) swelled EMel particles connected with these nanocarriers. $C_{\text{TBC2}} = 0.5 \text{ kg}\cdot\text{m}^{-3}$, $\varphi = 0.01 \text{ base}\cdot\text{mol}_{\text{EMel}}/\text{base}\cdot\text{mol}_{\text{PAAC}}$, pH = 3.0, $T = 20^\circ\text{C}$.

$\nu_{\text{asC=O}}$ vibration bands of -COO^- groups was fixed. It means that these -COO^- groups do not belong to zwitter-ions of EMel but can appear due to electrostatic interactions between acrylic acid units of the “corona”-forming PAAc blocks and amine groups of the EMel indol rings. Thus, basing on FTIR investigations, one can conclude that EMel encapsulation by DBC micelles contained in “coronas” PAAc blocks is realized mainly by means of electrostatic interactions. But in the case of TBC micelles with nonionic PEO “loops” in “coronas”, the process of EMel encapsulation proceeds mainly due to formation of different H-bonds between hydroxyl and/or uncharged carboxyl groups of the drug and oxygen atoms of PEO.

The confirmation of EMel connection with the copolymer micelles was obtained by TEM (Fig. 9). In these experiments we used the most stable TBC2 micelles.

Analysis of TEM images resulted in some important conclusions. Firstly, the studied EMel sample was not completely soluble in water at the selected pH value and comprised the swelled polydispersed nanoparticles. Moreover, at the EMel encapsulation its swelled nanoparticles were disposed at the micelle surface (Fig. 9b). Finally, the micelle size and morphology could change under influence of EMel encapsulation.

Conclusion

It is revealed the zwitter-ionic character of eumelanin macromolecules due to a presence the charged $>\text{NH}_2^+$ and -COO^- groups in a solid EMel sample, which is the vital activity product of black yeast “*Nadsoniella nigra* sp. X-1.” Polyampholyte properties of EMel were clearly displayed by potentiometric titration. So some excess (in 7 mol %) of secondary amine groups against carboxylic ones was determined. Acidic properties of both the groups were characterized. The values of pK_0 were equaled to 4.44 and 9.27 for carboxylic and amine groups consequently. Due to a strong compaction of melanin macromolecules, the appearance of insoluble fraction in aqueous medium was observed in the acidic region of the solution pH. Thus, it was shown that the state and solubility of melanin in aqueous medium is determined by a complex balance of electrostatic interactions and hydrogen bonds.

A wide spectrum of morphological forms of the MOPEO-*b*-PAAc and PAAc-*b*-PEO-*b*-PAAc micellar carriers could be produced by variation of the absolute and relative length of both the blocks. It was established that the DBC1 macromolecules formed spherical “crew-cut” micelles contained a small “corona” of short unbound segments of PAAc block. Unlike this, the DBC2 macromolecules formed the “hairy-type” micelles with a large developed “corona”, which comprised a significant excess of unbound PAAc units. In the cases of TBCs, the formation of “flower-like” micelles with a short “coronas” formed by “loops” of PEO central blocks was established.

The solubility of eumelanin sample at $\text{pH} \leq 6$ was ensured by its connection with MOPEO-*b*-PAAc and PAAc-*b*-PEO-*b*-PAAc micelles. It was revealed the essential influence a state of micellar systems, parameters of micellization process, sizes and morphology of micelles, nature and length of micellar “coronas” for EMel connection. In particular, the existence of evidently more developed hydrophilic “corona” in DBC2 “hairy-type” micelles resulted in the appearance of more stable in time EMel/DBC2 mixtures as compared to similar EMel mixtures with DBC1 “crew-cut” micelles containing a short “corona.” At the same time, free TBC2 “flower-like” micelles and their mixtures with EMel demonstrated higher stability in time than those formed by TBC1 sample. It was established that the encapsulation of EMel by the copolymer carriers took place due to electrostatic interactions and hydrogen bonds.

References

- [1] Torchilin, V.P. (2006). *Adv. Drug Deliv. Rev.*, 58, 1532.
- [2] Mozafari, M.R. (2007). *Nanomaterials and nanosystems for biomedical applications*, Springer: Dordrecht, the Netherlands.
- [3] Zheltonozhskaya, T., Partsevskaya, S. et al. (2013). *Europ. Polym. J.* 49, No.2, 405.
- [4] Oishi, M., & Nagasaki, Y. (2009). In: *Nanotechnology in drug delivery*, M.M. De Villiers et al. (Eds.), Chapter 2, Amer. Assoc. of Pharm. Scientists, Springer: New York, USA, 35.
- [5] Riess, G. (2003). *Prog. Polym. Sci.*, 28, 1107.
- [6] Kwon, G.S., & Forrest, M.L. (2006). *Drug Develop. Res.*, 67, 15.
- [7] Permyakova, N., Zheltonozhskaya, T. et al. (2012). *Macromol. Symp.*, 317–318, 63.
- [8] Permyakova, N.M., Zheltonozhskaya, T.B. et al. (2012). *J. of Proc. of the Inter. Conf. Nanomaterials: Application and Properties*, Alushta, the Crimea, Ukraine, 1, 01PCN37.
- [9] Permyakova, N., Zheltonozhskaya, T. et al. (2015). *Book of abstr. 8-th Int. Chemistry Conf. Toulouse-Kyiv*, 1–4 June, Toulouse, France, 99.
- [10] Schweitzer, A. D., Revskaya, E., Chu, P. et al. (2010). *Int. J. Radiat. Oncol. Biol. Phys.*, 78, № 5, 1494.
- [11] Huijser, A, Pezzellab, A., & Sundström, V. (2011). *Phys. Chem. Chem. Phys.*, 13, 9119.
- [12] Zonios G. Dimou, A. (2008). *Optics express*, 16, №11, 8263.
- [13] Corani, A., & Huijser, A. (2012). *J. Phys. Chem. B*, 116, 13151.
- [14] Chizhanska, N.V. (2008). In: *Investigation of the melanin antistress action mechanisms*, A thesis for the scientific degree of candidate of biological sciences, Kyiv, Ukraine, 125.
- [15] Zheltonozhskaya, T., Permyakova, N. et al. (2009). In: *Hydrogen-bonded interpolymer complexes. Formation, Structure and Applications*, Khutoryanskiy, V.V., Staikos, G. (Eds.) Chapter 5, World Scientific Publishing Company: Singapore-London-New-Jersey etc., 85.
- [16] Poe, G. D., Jarrett, W.L., Scales, C.W. et al. (2004). *Macromolecules*, 37, 2603.
- [17] Pretsch, E., Bullman, F., & Affolter, C. (2006). *Structure determination of organic compounds. Tables of spectroscopic data*. Moscow, Mir.
- [18] Zheltonozhskaya, T.B., Pop, G.S. et al. (1981). *Visokomol. Soed.*, 23, №11, 2425.
- [19] Holappa, S., Kantonen, L., Winnik, F., & Tenhu, H. (2004). *Macromolecules*, 37, 7008.
- [20] Shen, H., Zang, L., & Eisenberg, A. (1997). *J. Phys. Chem. B*, 101, 4697.
- [21] Alexandridis, P., & Hatton, T.A. (1996). In: *Block Copolymers. Polymer materials encyclopedia 1*, Boca Raton: CRC Press, 743.
- [22] Solomatin, S.V., Bronich, T.K., Bargar, T.W. et al. (2003). *Langmuir*, 19, 8069.